

Anticusp and binary peak structures in the electronic spectra arising from proton- and antiproton-helium collisions

C. O. Reinhold and D. R. Schultz

Department of Physics and Laboratory for Atomic and Molecular Research, University of Missouri–Rolla, Rolla, Missouri 65401

(Received 24 July 1989)

The spectra of electrons ejected in collisions of protons and antiprotons with helium at impact energies of 100 and 500 keV are reported and compared. These calculations extend recent studies of the electronic spectra by means of the classical-trajectory Monte Carlo method to consider more energetic ejected electrons. Specifically, these new calculations exhibit the well-known binary peak, around which protons and antiprotons are shown to yield similar results. On the other hand, as predicted by quantum-mechanical distorted-wave approximations, a clear dip or anticusp is found in the electronic spectra produced by antiproton impact at electron velocities close to the projectile velocity, unlike the enhancement or cusp found for proton impact. Our results are consistent with simple dynamical mechanisms that reflect the two-center nature of the collision.

I. INTRODUCTION

The experimental and theoretical study of the different structures appearing in the electronic spectra arising from collisions of completely stripped positive heavy ions with atoms has been the object of several works in the last decades. These works have revealed the presence of two well-known structures in the spectra of electrons ejected at forward angles which are usually known as the binary peak and the electron capture to the continuum (ECC) cusp.

The binary peak is the simplest structure in the electronic spectra since its shape and magnitude are predicted by simple first-order theories such as the classical binary-encounter model or the first Born approximation.^{1–3} For heavy-ion impact, this structure appears in the spectra as a peak or ridge that is observed at ejection angles $\theta < 90^\circ$ and electron energies around $E_b = 2m_e v^2 \cos^2 \theta$, m_e and v being the electron mass and the projectile velocity, respectively.

On the other hand, the ECC cusp is a sharp peak that is observed at very small ejection angles when the velocity of the ejected electrons is similar to that of the impinging projectile,^{4–6} i.e., the ECC peak is found when the energy of the ejected electrons is about $E_p = 0.5m_e v^2$. Even though the existence of this peak is predicted by first-order theories of capture to the continuum, its shape and magnitude can only be explained by more elaborated approximations which, to some extent, describe ionized electrons as electrons in the continuum of the combined projectile-target-nucleus field.

In recent years, theoretical studies of these structures have been undertaken for the case of antimatter projectiles.^{7–9} The appearance of these works is closely related to the advent of experimental measurements of electronic spectra arising from antimatter-atom collisions.¹⁰ These studies, together with studies of matter-atom collisions, provide a fundamental testing ground for theoretical ap-

proaches that go beyond simple first-order theories.

For example, according to first-order theories protons and antiprotons should produce the same electronic spectra. However, more elaborate theoretical studies of collisions of protons and antiprotons with helium have shown large departures from this simple scaling.^{7–9,11,12} For example, the study of Fainstein, Ponce, and Rivarola⁸ has indicated the existence of a dip or anticusp in the region of the spectra where the ECC peak is usually observed for impact of positively charged ions. Experimental evidence of this anticusp has recently been found by Yamazaki *et al.*¹⁰ in antiproton-carbon foil experiments.

Furthermore, Fainstein, Ponce, and Rivarola⁸ have found that protons and antiprotons yield similar cross sections around the binary peak. This conclusion is supported by the fact that even first-order theories, which predict the same cross sections for proton or antiproton impact, are expected to describe properly the binary peak.

Using the classical-trajectory Monte Carlo (CTMC) approximation,^{13,14} we present in this work further theoretical evidence that confirms previous general conclusions about the cusp or anticusp and binary structures in collisions of protons and antiprotons with helium. Use of this model provides an independent theoretical approach and illuminates the classical dynamics leading to the formation of these structures. Previous comparisons of the electronic spectra produced by proton or antiproton impact have been already performed using the CTMC method.^{11,12,15} However, due to the large computational effort required to observe these features, the anticusp and binary structures induced by antiproton impact were not directly observed. In addition, a detailed study of the ECC peak for incident protons has already been performed,^{11,16} but, for the same reason, no analysis of the binary peak was made. Moreover, we would like to note that, to our knowledge, the only prediction of the binary peak utilizing the CTMC method predating this work

was made by Bonsen and Banks¹⁷ in 1971 and was hampered by lack of sufficient computer resources.

II. RESULTS AND DISCUSSION

In Figs. 1 and 2 we display the results of our CTMC calculations of the doubly differential ionization cross sections arising from collisions of protons and antiprotons with helium at impact energies of 500 and 100 keV, respectively, for different ejection angles of 10°, 30°, and 50°, and as a function of the electron energy. Our results for incident protons are compared with the experimental data of Rudd, Toburen, and Stolterfoht.¹⁸ We also present theoretical calculations of the electronic spectra by means of the binary-encounter approximation³ which predicts the same cross section for both proton and antiproton impact, i.e., is independent of the sign of the charge of the projectile.

Figure 1 shows that at low electron energies the cross sections for proton impact are much higher than those for antiproton impact. At an ejection angle of 10°, the differences become larger as the electron energy increases and a clear dip appears for antiproton projectiles in the region where the electron energy is around $E_p = 272$ eV. This dip disappears as the ejection angle increases. The ECC peak for proton impact is not completely visible at 10°, but a remainder of this cusp can still be seen as a change in the slope of the differential cross section in the region where the dip is observed for antiproton impact.

The origin of these cusp or anticusp structures may be explained in terms of simple dynamical mechanisms. That is, the electrons that comprise these features arise from either a post-collision Coulomb focusing or defocusing depending on the sign of the projectile charge. As has been recently shown,¹¹ the focusing produced by a positively charged ion at intermediate impact energies and very small ejection angles extends to internuclear separations of thousands of atomic units and, further-

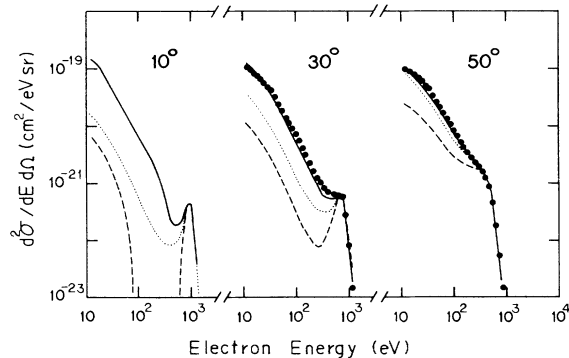


FIG. 1. Doubly differential cross section for ejection of electrons in collisions of protons (solid lines) and antiprotons (dashed lines) with He at an impact energy of 500 keV for ejection angles of 10°, 30°, and 50°, and as a function of the electron energy. The results for protons are compared with the experimental data of Rudd, Toburen, and Stolterfoht (Ref. 18, Table V) (closed circles) normalized to the total cross section of Shah and Gilbody (Ref. 19). The dotted lines indicate the cross sections predicted by the binary-encounter approximation.

more, that the interaction of the electron with the residual target nucleus is not negligible. Since the anticusp is characterized by a lack of electrons with energies around E_p , with the presently available statistics of our simulation we have not been able to make a meaningful estimate of the range of the antiproton defocusing, but expect a result similar to the range of the focusing at very small ejection angles.

At electron energies higher than E_p , our calculations exhibit very clearly the well-known binary peak where protons and antiprotons yield similar cross sections. At 30° this peak becomes a shoulder around which our calculations for protons are in very good agreement with the experimental data of Rudd, Toburen, and Stolterfoht.¹⁷

Figure 2 shows that similar conclusions are obtained at an impact energy of 100 keV. However, we note that the differences between the yield of electrons induced by proton or antiproton impact becomes greater and the dip becomes much deeper. We also note that at this impact energy the binary peak for proton impact is completely hidden in the electronic spectra, in agreement with the experimental data. Furthermore, differences between proton and antiproton impact exist for electron energies greater than that of the binary peak, the cross sections for antiprotons being greater than those for protons.

As has previously been discussed,^{8,11} the reason for the differences between the electronic spectra produced by either proton or antiproton impact lies in the two-center nature of the ionization problem. This fact is illustrated very clearly in Fig. 3, where we display the ratio between the cross sections produced by these projectiles as a function of the electron energy in units of the ECC peak position E_p . According to single-scattering or first-order theories such as the binary encounter or the first Born approximations, the ratio should be equal to 1. However, large differences from this value, ranging from a factor of 10 to a factor of 10^{-3} , are displayed.

These differences can be easily explained in terms of the differences between the collision dynamics for impact of either a positively or a negatively charged ion. In the case of production of soft electrons, the main difference between the collision dynamics for proton or antiproton

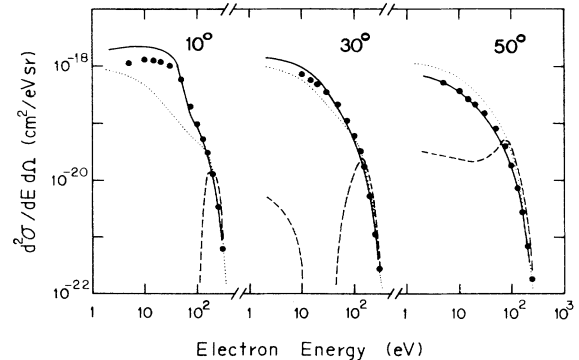


FIG. 2. Same as in Fig. 1, but at an impact energy of 100 keV. The results for protons are compared with the absolute experimental data of Rudd, Toburen, and Stolterfoht (Ref. 18, Table I) (closed circles).

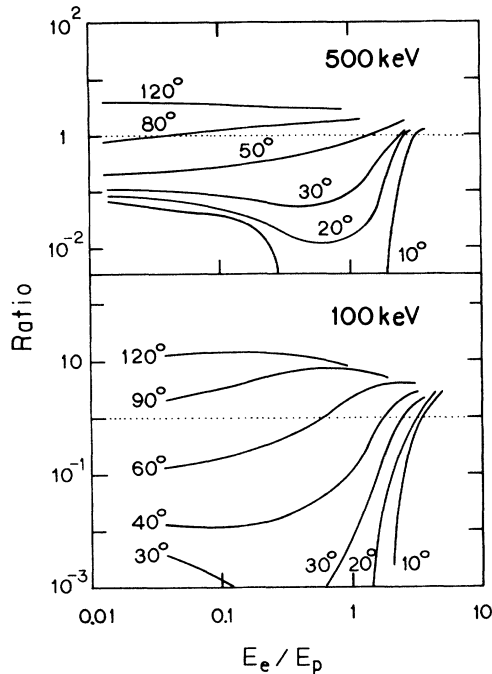


FIG. 3. Ratio of the doubly differential cross sections for antiproton impact of helium to those for proton impact at collision energies of 100 and 500 keV, for different ejection angles and as a function of the ratio of the electron energy to the ECC peak energy E_p . The horizontal dotted lines indicate the ratio predicted by first-order theories such as the binary encounter or the first Born approximation.

impact is that while protons pull out electrons to small angles, antiprotons push them to larger angles. This difference becomes critical at small ejection angles and electron energies around E_p where protons focus the ejected electrons whereas antiprotons repel them to larger angles and/or different energies.

Surprisingly, the differences between proton or antiproton impact persist even at electron energies above that of the binary ridge. While this electron energy range is usually associated with a binary-collision mechanism that should not depend on the sign of the projectile charge, our ratios tend to a value greater than one which seems to be independent of the ejection angle, in agreement with the calculations of Fainstein, Ponce, and Rivarola.⁸ In fact, analysis of individual CTMC trajectories has indicated that fast electrons originate from very close and strong interactions between the electron and the projectile. However, the differences observed in the rate of production of fast electrons indicate that the interaction between the active electron and the target nucleus plays a significant role in the collision dynamics.

Fainstein, Ponce, and Rivarola⁸ suggested that the differences found for fast electrons could be related to the differences existing between the ionization probabilities for proton and antiproton impact at impact parameters smaller than the radius of the initial electronic cloud.²⁰ However, we have verified that the ionization probabilities for proton or antiproton impact differ in an amount that is too small to account for these differences. In addition, we have found that fast electrons originate from collisions with a wide range of intermediate impact parameters and that, consequently, a close encounter between the electron and the projectile does not necessarily imply a very small impact parameter. Therefore we conclude that the impact parameter does not provide a decisive description of the differences obtained for fast electrons.

We find that the differences at high ejection energies arise from a screening or antiscreening effect due to the varying sign of the projectile charge. That is, for protons, a larger net nuclear charge is experienced by the escaping high-energy electron than in the case of antiproton impact, where the residual nuclear charge is partially screened. Thus hot electrons ejected in antiproton impact may attain higher kinetic energies because they escape from a lower net nuclear charge. Thus this difference on the high-energy side of the binary peak is a simple consequence of the two-center nature of the collision.

Finally, we note that we have found some disagreements between our results and those obtained by Fainstein, Ponce, and Rivarola⁸ as to the magnitude of the differences between the cross sections for proton or antiproton impact. These authors have calculated the ratio of the cross section for antiproton impact to that for proton impact at 0.3 and 1 MeV. The major difference is found at small ejection angles and small electron energies where our ratios are smaller than 0.1 whereas the ratios of these authors are greater than 0.5. Future measurements of the electronic spectra produced by proton and antiproton impact may determine conclusively the magnitude of these ratios.

Thus our calculations of the electronic spectra arising from proton and antiproton impact of helium, using a semiclassical, nonperturbative approach (CTMC), confirm and extend the previous general conclusions obtained in the analysis of the anticusp and binary peak structures with the quantum-mechanical, perturbative method of Fainstein, Ponce, and Rivarola.⁸

ACKNOWLEDGMENTS

The authors would like to acknowledge both Dr. Ronald E. Olson and the Office of Fusion Research, U.S. Department of Energy for their support.

¹M. E. Rudd and T. Jorgensen, *Phys. Rev.* **131**, 666 (1963).

²M. E. Rudd, C. A. Sauter, and C. L. Bailey, *Phys. Rev.* **151**, 20 (1966).

³T. F. M. Bensen and L. Vriens, *Physica* **47**, 307 (1970).

⁴G. B. Crooks and M. E. Rudd, *Phys. Rev. Lett.* **25**, 1599 (1970).

⁵A. Salin, *J. Phys. B* **2**, 631 (1969); **2**, 1225 (1969).

⁶J. H. Macek, *Phys. Rev. A* **1**, 235 (1970).

⁷C. R. Garibotti and J. E. Miraglia, *Phys. Rev. A* **21**, 572 (1980).

- ⁸P. D. Fainstein, V. H. Ponce, and R. D. Rivarola, *J. Phys. B* **21**, 2989 (1988).
- ⁹M. Brauner and J. S. Briggs, *J. Phys. B* **19**, L325 (1986).
- ¹⁰Y. Yamazaki, K. Kuroki, F. Fujimoto, L. H. Andersen, P. Hvelplund, H. Knudsen, S. P. Moller, E. Uggerhoj, and K. Elsener (unpublished).
- ¹¹C. O. Reinhold and R. E. Olson, *Phys. Rev. A* **39**, 3861 (1989).
- ¹²R. E. Olson and T. J. Gay, *Phys. Rev. Lett.* **61**, 302 (1988).
- ¹³R. Abrines and I. C. Percival, *Proc. Phys. Soc.* **88**, 861 (1966).
- ¹⁴R. E. Olson and A. Salop, *Phys. Rev. A* **16**, 531 (1977).
- ¹⁵D. R. Schultz, C. O. Reinhold, and R. E. Olson, *Nucl. Instrum. Methods B* **42**, 527 (1989).
- ¹⁶C. O. Reinhold and R. E. Olson, *J. Phys. B* **22**, L39 (1989).
- ¹⁷T. F. M. Bensen and O. Banks, *J. Phys. B* **4**, 706 (1971).
- ¹⁸M. E. Rudd, L. H. Toburen, and N. Stolterfoht, *At. Data Nucl. Data Tables* **18**, 413 (1976).
- ¹⁹M. B. Shah and H. B. Gilbody, *J. Phys. B* **18**, 899 (1985).
- ²⁰R. E. Olson, *Phys. Rev. A* **36**, 1519 (1987).